Contribution from the Department of Biophysics, Institute of Molecular Biology, Jagiellonian University, 31-120 Krakow, Poland, Department of Chemistry, University of Siena, 53100 Siena, Italy, and National Biomedical ESR Center, Medical College of Wisconsin, Milwaukee, Wisconsin 53226

Multifrequency ESR with Fourier Analysis of $Cu^{II}(His)_n$ (His = Histidine). 2. Mobile Phase[1]

Marta Pasenkiewicz-Gierula,[†§] Wojciech Froncisz,[†§] Riccardo Basosi,[‡§] William E. Antholine,*[§] and James S. Hyde[§]

Received May 27, 1986

Mobile-phase $Cu(His)_2$ complexes in water at room temperature in the presence of excess histidine are characterized by ESR methods. In order to identify the nitrogen donor atom, histidine, for which ^{14}N in the imidazole ring is substituted with ^{15}N, was used. Spectra in the presence of excess histidine have been analyzed by simulation of second-derivative spectra and by Fourier and reverse Fourier transforms of the spectra. It is concluded that the spectra arise from a superposition of an 80% contribution from complexes formed with two histidines in a histamine-like configuration and a 20% contribution from complexes with two histidines: one glycine-like and one histamine-like. It is suggested that Fourier and reverse Fourier transforms are particularly effective methods to analyze the nitrogen superhyperfine patterns in spectra from copper–histidine complexes.

Introduction

Copper exists in the body both in copper proteins and in low molecular weight complexes. This paper is concerned with complexes of copper with histidine. Such complexes are known to exist in the body, but they are not the dominant species under any conditions, to our knowledge, and their role remains unknown. Most extracellular copper is not incorporated into histidine but into ceruloplasmin. Serum albumin, not histidine, is the most readily available source of copper for tissues. Metallothionein appears to store intracellular cuprous ion whereas superoxide dismutase and cytochrome *c* oxidase are two of many enzymes that utilize copper and may also store copper. Yet, the binding of cupric ion to histidine may have important biological implications.[2]

Even though copper histidine complexes account for less than 19% of plasma copper, they may contribute to the absorption of copper in the gut and the transport of copper. Whether these are essential to these functions is not well understood. However, there exists a body of literature in which addition of histidine is shown to facilitate transport of copper to tissues.[2]

It is also likely that cupric ion binds the monodentate imidazole moiety. For example, the tripeptide GHL, N^2-(*N*-glycyl-L-histidyl)-L-lysine, is isolated with copper from human plasma. CuGHL enhances the growth and survival of cultured hepatoma cells and hepatocytes whereas cupric salts decrease the number of cultured cells.[3] Copper is bound to this tripeptide, GHL, through an amine, a peptide nitrogen, and an imidazole nitrogen much as cupric ion is bound to serum albumin and the β chain of hemoglobin.[4,5] Whether ligand binding is altered upon freezing for cupric ion bound to low molecular weight peptides like the drug bleomycin[6] or to high molecular weight proteins such as serum albumin[5] and hemoglobin is an unsolved question.[7] Before addressing this question concerning the binding of the monodentate imidazole moiety, it seemed important to determine whether the structure for cupric ion bound to excess histidine can be altered during the freezing process.

It is clear from our recent ESR studies that cupric ion in the presence of excess histidine will bind to four equivalent nitrogen donor atoms from the imidazole moiety of histidine in frozen solutions.[8] This constitutes a stoichiometry of $Cu(His)_4$. The binding of four histidines was surprising because histidine in solution is a tridentate ligand that acts as a bidentate ligand; log K_1 = 10.2 and log K_2 = 7.9.[9] Thus there appears to be large changes in coordination for cupric ion in the presence of excess histidine as the solution freezes. In this report we have reinvestigated the bidentate binding of excess histidine to cupric ion in solution using the ESR method and have tried to determine the changes in ligand binding upon freezing.

In order to determine whether the imidazole and the amine are bound to cupric ion, ESR spectra for cupric ion in the presence of excess histidine in which ^{15}N is substituted for ^{14}N only in the imidazole ring are compared to ESR spectra for cupric ion in the presence of excess histidine where naturally abundant ^{14}N exists in both the amine and the imidazole ring. However, the nitrogen hyperfine structure for the ^{15}N-substituted histidine is not well resolved. Fourier transform analysis of ESR spectra of cupric ion helped determine that both ^{14}N and ^{15}N are bound to cupric ion in solution, but only ^{15}N is bound in the frozen state. Thus, it is reassuring that histamine-like or mixed histamine-like and glycine-like complexes are formed in solution. These ESR data agree in substance but not in all details with the analysis of the ESR data of Goodman et al.[10] These authors were the first to detect nitrogen superhyperfine structure on the high-field line for $Cu(His)_2$ in D_2O using second-derivative spectra. They suggest a mixture of copper complexes consisting of 50% of a complex with three nitrogen donor atoms and 50% of a complex with four nitrogen donor atoms. In this paper improved methods and improved computer simulations characterize the nitrogen superhyperfine structure of copper histidine spectra. Isotope substitution of ^{15}N for ^{14}N in the imidazole ring of histidine, Fourier transforms (actually significance plots) of the spectra, and reverse Fourier transforms of the spectra indicate that the predominant species in the liquid phase in all cases is the histamine-like structure for both histidine ligands.

Experimental Section

L-His from Merck and DL-His-*1,3*-$^{15}N_2$ from MSD isotopes were used without further purification. The solutions were made in 99.75% D_2O, from Merck, and the uncorrected pD was adjusted with either DCl or NaOD. Isotopically pure ^{63}Cu (from Oak Ridge National Laboratory) was used for these ESR experiments.

X-Band ESR spectra (ν = 9.1 GHz) were obtained with a Varian E-109 Century Series X-band spectrometer. (The ESR facilities are located at the NIH-sponsored National Biomedial ESR Center at the

* To whom correspondence should be addressed.
† Jagiellonian University.
‡ University of Siena.
§ Medical College of Wisconsin.

(1) This work was supported by NIH Grant GM35472 and by the National Biomedical ESR Center through NIH Grant RR01008.
(2) Ettinger, M. J. In *Copper Proteins and Coppery Enzymes*; Lontie, R., Ed.; CRC Press: Boca Raton, FL, 1984; Vol. III, pp 176–190.
(3) Pickart, L.; Goodwin, W. H.; Burgua, W.; Murphy, T. B.; Johnson, D. K. *Biochem. Pharm.* **1983**, *32*, 3868.
(4) Rakhit, G.; Antholine, W. E.; Froncisz, W.; Hyde, J. S.; Pilbrow, J. R.; Sinclair, G. R.; Sarkar, B. *J. Inorg. Biochem.* **1985**, *25*, 217–224.
(5) Rifkind, J. M. *Met. Ions Biol. Syst.* **1981**, *12*, 191–232.
(6) Antholine, W. E.; Riedy, G.; Hyde, J. S.; Basosi, R.; Petering, D. H. *J. Biomol. Struct. Dyn.* **1984**, *2*, 469–480.
(7) Antholine, W. E.; Taketa, F.; Wang, J. T.; Manoharan, P. T.; Rifkind, J. M. *J. Inorg. Biochem.* **1985**, *25*, 95–108.
(8) Basosi, R.; Valensin, G.; Gaggelli, E.; Froncisz, W.; Pasenkiewicz-Gierula, M.; Antholine, W. E.; Hyde, J. S. *Inorg. Chem.* **1986**, *25*, 3006–3010.
(9) Martin, R. B. *Met. Ions Biol. Syst.* **1979**, *9*, 7.
(10) Goodman, B. A.; McPhail, D. B.; Powell, H. K. *J. Chem. Soc., Dalton Trans.* **1981**, 822–827.

0020-1669/87/1326-0801$01.50/0

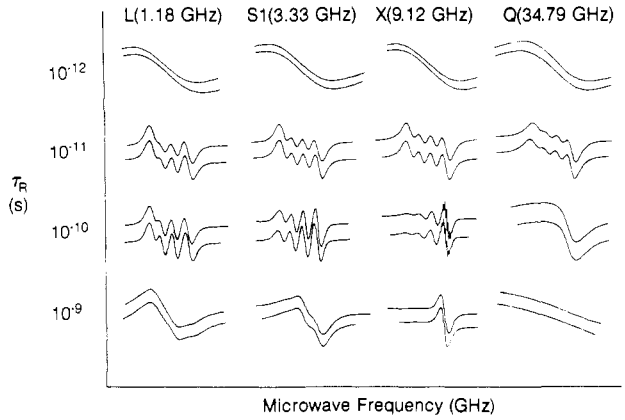

Figure 1. Display of computer-simulated spectra for ^{63}Cu(L-His)$_2$ at four microwave ESR frequencies and four widely varying correlation times. The top spectrum for each series has been plotted with the representative ESR parameters $g_\parallel = 2.220$, $g_\perp = 2.034$, and $A_{iso} = 65$ G for four equivalent nitrogen donor atoms ($a_N = 13.5$ G). Each simulated spectrum is compared with the homologous spectrum (bottom) obtained with three equivalent nitrogens ($a_N = 13.5$ G).

Medical College of Wisconsin.) Microwave frequencies were measured with an EiP model 331 counter, and the magnetic field was calibrated with a MJ-110R Radiopan NMR magnetometer. Samples were contained in an ESR flat cell.

The X-band ESR spectrum for Cu(His)$_2$ was simulated by using a program written by W.F. for a fast-tumbling copper complex in an isotropic environment. The program is based on Kivelson's theory taking into account the line width equations of Kivelson,[11-14] the second-order frequency shift equation of Bruno et al.,[15] and the further assumption of Lorentzian line shapes.[16] ESR spectra were simulated by using a Monte Carlo method. Selected spectral parameters were randomly varied within defined limits and χ^2 was calculated with respect to the experimental spectrum for each set of parameters. The initial ESR parameters were taken from the literature[10] and spectral inspection.

Fourier transforms of ESR spectra were calculated with an IBM computer using a "fast Fourier transform" program. The spectra are, of course, real functions. A significance plot for each spectrum was formed according to Brumby[17] in which $[Re^2 + Im^2]^{1/2}$ is displayed on a graphic terminal where Re and Im are the real and imaginary parts of the FT. This display is a convenient one by which the spectroscopist on the basis of his specialized knowledge can decide to delete selected features. After the values in Re and Im that correspond to these features are set to zero, the reverse FT is calculated. It remains real. All field-swept spectra were digitized at 512 points and mapped one to one into points in FT space.

Results

It is apparent from the spectra in Figure 1 that the line position and line width of Cu(His)$_2$-like complexes vary with the rotational correlation time, τ_R, and microwave frequency. The correlation time corresponds to a molecular weight consistent with Cu(His)$_2$. The spectra in Figure 1 were then simulated by using representative parameters for a Cu(His)$_2$-like complex and assuming either four nitrogens (upper spectrum for the pair) or three nitrogens coordinated to copper ion. The coordination of four nitrogen donor atoms as opposed to three nitrogen donor atoms is usually difficult to determine. The line shapes for three or four nitrogens are very similar (Figure 1). For unresolved hyperfine structure the intensity of the line drops off more rapidly in the wings for three approximately equivalent nitrogen donor atoms than for four nitrogen donor atoms. The wing intensities are not used very often to determine the number of nitrogen donor atoms because the differences are small. It is best to do this type of line shape analysis by using the second-derivative display of a single

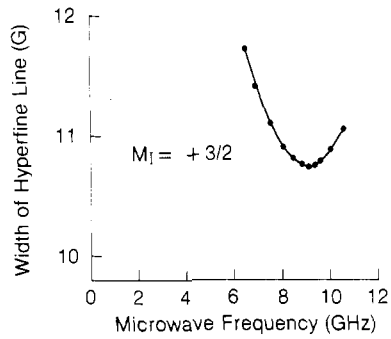

Figure 2. Computed superhyperfine width for the high-field $M_I = +^3/_2$ hyperfine line of the ESR spectrum of the ^{63}Cu(L-His)$_2$ complex vs. microwave frequency (ESR parameters given in the caption for Figure 1).

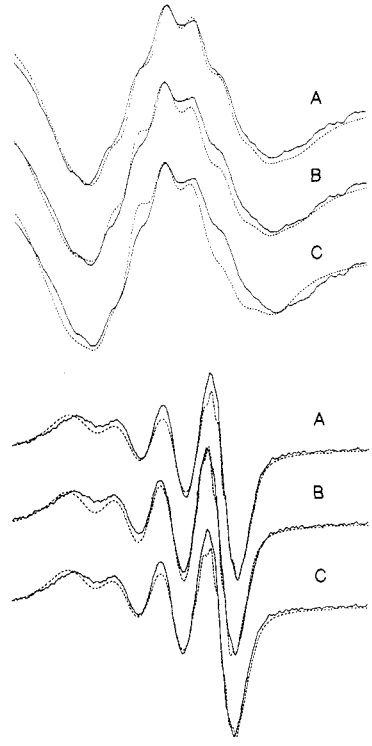

Figure 3. Top three spectra: second-derivative, X-band, ESR spectra (solid lines) for the $M_I = +^3/_2$ line for $^{63}Cu^{2+}$ (2 mM) in the presence of excess histidine (20 mM) in D_2O at room temperature; simulated spectra (dashed lines) assuming four nitrogen donor atoms, ^{63}Cu-4N (C), three nitrogen donor atoms, ^{63}Cu-3N (B), and 80% relative concentration for a complex with four nitrogen donor atoms superimposed with 20% for a complex with three nitrogen donor atoms (A). ESR parameters are as shown below. Bottom three spectra: first-derivative, X-band ESR spectra (solid lines) showing all lines for $^{63}Cu^{2+}$ (2 mM) in the presence of excess histidine (20 mM) in D_2O at room temperature; simulated spectra (dashed lines) assuming a superposition of 80% Cu-4N plus 20% Cu-3N (A), 100% Cu-3N (B), and 100% Cu-4N (C).

		g	A^{Cu}, G	A^N, G	line width, G
^{63}Cu-3N	$\perp$	2.04383	15.80	11.10	9.00
	$\parallel$	2.20533	153.20	11.10	9.00
	iso	2.09800	61.50		
	Δ	0.16250	137.40		
	τ = 85.00 ps; mol fract = 0.200				
^{63}Cu-4N	$\perp$	2.05133	13.93	11.00	9.00
	$\parallel$	2.21083	156.93	11.00	9.00
	iso	2.10450	61.60		
	Δ	0.15950	143.00		
	τ = 85.00 ps; mol fract = 0.800				

(11) Kivelson, D. *J. Chem. Phys.* **1957**, *27*, 1087–1098.
(12) Kivelson, D. *J. Chem. Phys.* **1960**, *33*, 1094–1106.
(13) Kivelson, D. *J. Chem. Phys.* **1964**, *41*, 1904–1909.
(14) Wilson, R.; Kivelson, D. *J. Chem. Phys.* **1966**, *44*, 154–168.
(15) Bruno, G. V.; Harrington, J. K.; Eastman, M. P. *J. Phys. Chem.* **1977**, *81*, 1111–1117.
(16) Basosi, R.; Antholine, W. E.; Froncisz, W.; Hyde, J. S. *J. Chem. Phys.* **1984**, *81*, 4849–4857.
(17) Brumby, S. *J. Magn. Reson.* **1979**, *35*, 357–465.

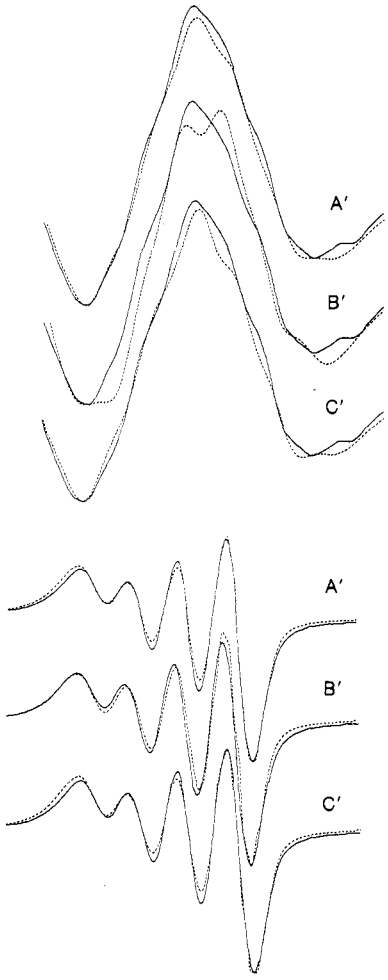

Figure 4. Top three spectra: second-derivative, X-band ESR spectra (solid lines) at room temperature in D_2O for the $M_I = +^3/_2$ line for $^{63}Cu^{2+}$ (2 mM) in the presence of excess histidine-*1,3*-$^{15}N_2$ for which the ^{15}N isotope is substituted for ^{14}N in the imidazole ring; simulated spectra (dashed lines) assuming two ^{14}N donor atoms plus two ^{15}N donor atoms, ^{63}Cu-$2^{14}N,2^{15}N$ (C'), two ^{14}N donor atoms plus one ^{15}N donor atom, ^{63}Cu-$2^{14}N,^{15}N$ (B'), and 80% relative concentration for ^{63}Cu-$2^{14}N,2^{15}N$ superimposed with 20% for ^{63}Cu-$2^{14}N,^{15}N$ (A'). Bottom three spectra: first-derivative, X-band, ESR spectra (solid lines) showing all lines for $^{63}Cu^{2+}$ (2 mM) in the presence of excess histidine-*1,3*-$^{15}N_2$ in D_2O at room temperature; simulated spectra (dashed lines) assuming a superposition of 80% ^{63}Cu-$2^{14}N,2^{15}N$ plus 20% ^{63}Cu-$2^{14}N,^{15}N$ (A'), 100% ^{63}Cu-$2^{14}N,^{15}N$ (B'), and 100% ^{63}Cu-$2^{14}N,2^{15}N$ (C'). ESR parameters are given in the caption for Figure 3 except $^{15}N = 1.4 \times {}^{14}N$.

hyperfine line, for example, the high-field $+^3/_2$ line, and expand the scale to maximum height and width.[10] If the hyperfine structure is resolved, the number of nitrogen donor atoms may be determined from this pattern. There exists an optimum frequency to minimize the line width.[18,19] The frequency that gives the best resolution for the high-field line is 9.1 GHz (Figures 1 and 2). Figure 1 shows that the resolution of the high-field line is only observed for $\tau_R \sim 10^{-10}$ s. By the procedure of Goodman et al.[10] well-resolved spectra for ^{63}Cu in the presence of excess histidine in D_2O were simulated for three models: four equivalent ^{14}N donor atoms, Cu-$4^{14}N$; three equivalent ^{14}N donor atoms, Cu-$3^{14}N$; or a mixture of Cu-$4^{14}N$ and Cu-$3^{14}N$ (Figure 3). A good fit was obtained for the entire spectrum for the model with two complexes by using the first-derivative display (Figure 3) and for the three high-field lines (but not the low-field line) by using the second-derivative display (data not shown). This fit consisted of a superposition of the spectrum for Cu-$4^{14}N$ (80%) and Cu-$3^{14}N$ (20%), where the τ_R value is 85 ps for both complexes. In order

(18) Hyde, J. S.; Froncisz, W. *Annu. Rev. Biophys. Bioeng.* **1982**, *11*, 391–417.
(19) Froncisz, W.; Hyde, J. S. *J. Chem. Phys.* **1980**, *73*, 3123–3131.

Table I. ^{14}N and ^{15}N Hyperfine Coupling Constants for the $M_I = -^1/_2$ Line in the $g_\parallel$ Region

donor atoms	pattern[a]
$1^{14}N$	1-1-1
$2^{14}N$	1-2-3-2-1
$3^{14}N$	1-3-6-7-6-3-1
$4^{14}N$	1-4-10-16-19-16-10-4-1
$1^{15}N$	1--1
$2^{15}N$	1--2--1
$3^{15}N$	1--3--3--1
$4^{15}N$	1--4--6--4--1
$1^{14}N + 1^{15}N$	1--1--1-1--1--1
$2^{14}N + 1^{15}N$	1--2-1-3-2-2-3-1-2--1
$1^{14}N + 2^{15}N$	1--1-2--1-2-1--2-1--1
$2^{14}N + 2^{15}N$	1--2-2-3-4-1-2-6-2-1-4-3-2-2--1

[a] The ratio of the moments for ^{15}N to ^{14}N is about 1.4.

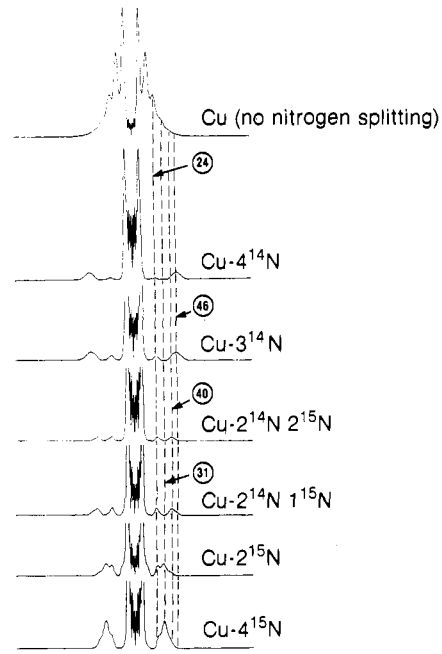

Figure 5. Fourier transform amplitude spectra (significance plots) for simulated spectra for which ESR parameters are given in the caption for Figure 3. The spectra are plotted as intensity vs. position number. In this figure there are 512 positions for the magnetic field, which correspond one to one to Fourier transform space. Transforms from top to bottom are for the following simulations: Cupric complex with no nitrogen donor atoms, with four ^{14}N donor atoms, with three ^{14}N donor atoms, with two ^{14}N plus two ^{15}N donor atoms, with two ^{14}N plus one ^{15}N donor atoms, with two ^{15}N donor atoms, and with four ^{15}N donor atoms. The four vertical dashed lines from left to right indicate the 24th, 31st, 40th, and 46th positions.

to simulate the ESR spectrum of copper in the presence of excess histidine in which ^{15}N is substituted for ^{14}N only in the imidazole ring, the same ESR parameters were used as given in Figure 3, except the hyperfine splitting constant for ^{15}N was 1.4 times the hyperfine splitting for ^{14}N and the hyperfine patterns were altered as shown in Table I. The same three models were tested. The best fit was obtained for the model having two complexes: Cu-$2^{14}N,2^{15}N$ (80%) and Cu-$2^{14}N,^{15}N$ (20%) with $\tau_R = 65$ ps (Figure 4).

That the nitrogen hyperfine coupling pattern for cupric ion in the presence of excess histidine arises from predominantly a single complex containing both ^{15}N and ^{14}N donor atoms is even more apparent from the significance plot of the ESR spectra (Figures 5 and 6). In the Fourier transform domain, the model spectra differ with respect to the positions of the lines according to a change in the hyperfine pattern (Figure 5 and Table I). Patterns for ^{14}N, which have an 11-G hyperfine coupling constant, correspond to the outermost lines at the 46th position in the Fourier transform domain. ^{63}Cu, with a hyperfine splitting of 61 G,

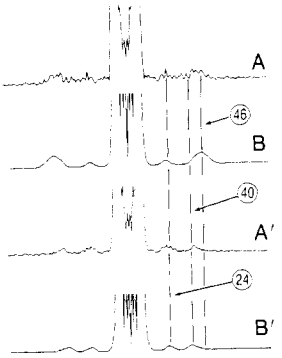

Figure 6. Fourier transform for experimental data for ^{63}Cu in the presence of excess histidine, Cu-^{14}N-exptl (A); transform for simulated data assuming 80% relative concentration of a cupric complex with four ^{14}N nitrogen donor atoms, Cu-4^{14}N, and 20% with three ^{14}N nitrogen donor atoms, Cu-3^{14}N (B); transform for experimental data for ^{63}Cu in the presence of excess histidine-*1,3*-$^{15}N_2$ (A'); and transform for simulated data assuming 80% concentration of a cupric complex with two ^{14}N and two ^{15}N nitrogen donor atoms, Cu-2^{14}N,2^{15}N, and 20% Cu-2^{14}N,^{15}N (B').

corresponds to the 8th position. Higher harmonics of the copper line are at the 16th and 24th positions (see the top spectrum in Figure 5). If a mixture of ^{14}N and ^{15}N donor atoms forms the square-planar configuration, lines at the 46th and 31st positions in the frequency domain are absent and a line at the 40th position appears.

Several points can be drawn from the Fourier transforms in Figure 5. First, there is little overlap between the position for ^{14}N and positions for ^{15}N or Cu. Second, there is some overlap between the 31st position for ^{15}N and the 3rd harmonic for copper at position 24. Third, there is a shift to a lower position (position 40) if a mixtue of ^{14}N and ^{15}N contributes to the square-planar configuration. If the spectra for a mixture of two complexes, one with only ^{14}N donor atoms and one with only ^{15}N donor atoms, are superimposed, lines at the 46th and 31st positions (not at the 40th position) confirm the absence of a complex with both ^{14}N and ^{15}N donor atoms (data not shown).

In the Fourier transform domain, the ESR spectra for ^{63}Cu in the presence of excess histidine are similar to the simulated spectrum composed of 80% by concentration of cupric ion bound to four nitrogen donor atoms, Cu-4^{14}N, and 20% of a cupric complex bound to three nitrogen donor atoms, Cu-3^{14}N (Figure 6). The ESR spectrum for ^{63}Cu in the presence of excess histidine with ^{15}N in the imidazole ring, Cu-^{14}N,^{15}N, is similar to the spectrum composed of 80% cupric ion bound to two ^{15}N donor atoms plus two ^{14}N donor atoms, Cu-2^{14}N,2^{15}N, and 20% of cupric ion bound to one ^{15}N plus two ^{14}N donor atoms, Cu-2^{14}N,^{15}N. It is not surprising that the spectral fits in Figures 3 and 4 complement the fits for the Fourier transform domain in Figure 6. But, it is more apparent from the shift in the peaks in the Fourier transform display that both ^{14}N and ^{15}N are donor atoms.

The patterns from the reverse Fourier transform of spectra, for which all lines except the one at position 46 or 40 in the Fourier transform domain were cut out for both experimental and model spectra, correspond to the nitrogen hyperfine splitting patterns for Cu-4^{14}N or Cu-2^{14}N,2^{15}N (Figure 7A,A',B,B') or for Cu-3^{14}N or Cu-2^{14}N,^{15}N (Figure 7C,C'). The second-derivative patterns (Figure 7) relate to the appropriate stick diagrams (Table I) and to the second-derivative experimental and simulated spectra (Figures 3 and 4). The positions and amplitudes for the reverse Fourier transform of the experimental spectrum correlate with the model, 80% Cu-4^{14}N and 20% Cu-3^{14}N or 80% Cu-2^{14}N,2^{15}N and 20% Cu-2^{14}N,^{15}N (see dashed lines, Figure 7). Only the left sides of the simulated reverse transforms overlap with the experimental reverse transforms. The right side is distorted because of extra oscillations in the experimental line that overlap with the right-hand side more than the left-hand side (see base line Figure 7A,A'). The pattern for the simulated transform with 80% Cu-2^{14}N,2^{15}N has the same odd symmetry, whereas the pattern for Cu-2^{14}N,^{15}N has even symmetry (Figure 7A',B',C' and Table I). Since the line widths in the experimental spectra are about 9 G as determined from simulations, the hyperfine lines from the copper splitting begin to overlap. A simplified simulation was constructed from the stick diagrams for 2^{14}N,2^{15}N; 2^{14}N,^{15}N; and 2^{14}N assuming $a(^{14}N)$ = 10 G and $a(^{15}N)$ = 14 G by convolution with a 10-G Gaussian line. Figure 8 shows the stick diagrams before and after convolution and the amplitude spectrum in the Fourier transform domain. Usually three interpretable peaks are observed for the amplitude spectrum: a central peak representing the entire shape of the spectrum, peaks at about the 25th–28th positions attributed to higher harmonics of the entire spectrum, and peaks at the 43rd–49th positions representing the dominant separation between the hyperfine lines. The pattern for the nitrogen hyperfine structure (Table I) is contained in the outermost peaks (Figure 8). An odd pattern consisting of seven lines is obtained from the reverse Fourier transform for the 2^{14}N,2^{15}N

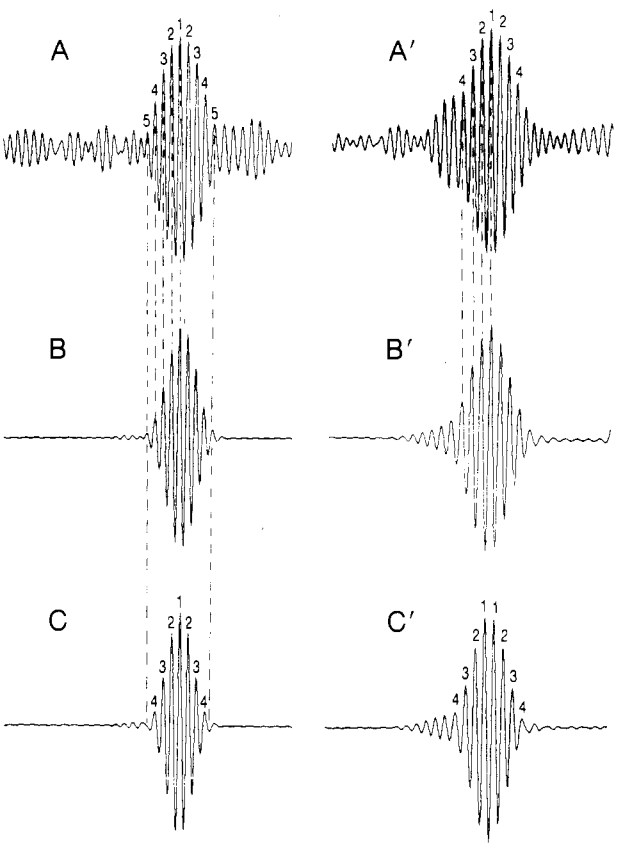

Figure 7. Second-derivative pattern of the reverse Fourier transform taken from the high-frequency position of the transform for Cu-^{14}N-exptl (A), for the simulated spectrum with 80% Cu-4^{14}N plus 20% Cu-3^{14}N (B), for the simulated spectrum of Cu-3^{14}N (C), for Cu-^{14}N,^{15}N-exptl (A'), for the simulated spectrum with 80% Cu-2^{14}N,2^{15}N plus 20% Cu-2^{14}N,^{15}N (B'), and for the simulated spectrum of Cu-2^{14}N,^{15}N (C').

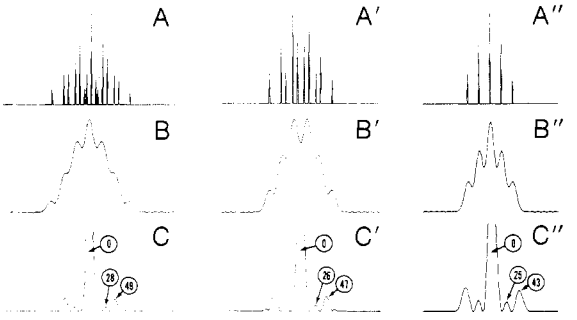

Figure 8. Stick diagram, convoluted stick diagram with Lorentzian line shape, and reverse Fourier transform for models Cu-2^{14}N,2^{15}N (A, B, C), Cu-2^{14}N,^{15}N (A', B', C'), and Cu-2^{14}N (A'', B'', C''). Lines for the complex Cu-2^{14}N are presented for comparison to a mixed complex with both ^{14}N and ^{15}N donor atoms and a complex with only ^{14}N donor atoms.

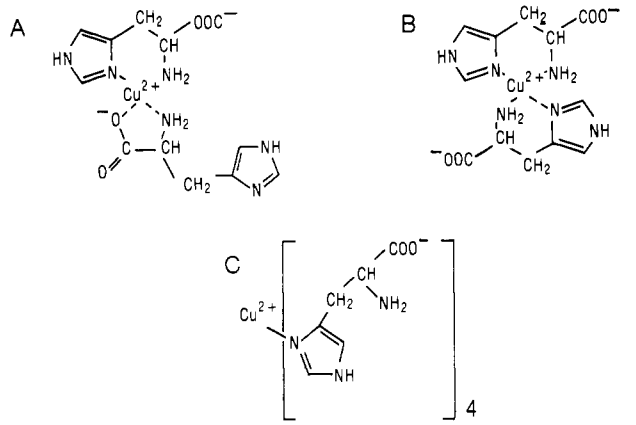

Figure 9. Structures for Cu(L-His)$_n$ complexes in aqueous solution at pH 7.3.

pattern and an even pattern for $2^{14}N,^{15}N$. Thus the resolution for the reverse Fourier transform is adequate to confirm that the odd pattern for $2^{14}N,2^{15}N$ dominates the spectrum for cupric ion in the presence of excess histidine-*1,3*-$^{15}N_2$.

Discussion

Copper in the presence of excess histidine in frozen solutions is bound to four nitrogens from the imidazole ring of histidine, forming a nearly square-planar complex (Figure 9c).[8] The present studies establish that a mixture of a histamine-like and glycine-like structures (Figure 9a,b) exists in the liquid phase. Our original purpose for the addition of excess histidine was to prevent aggregation of the sample upon freezing without affecting axial coordination from substances like perchlorate, dimethyl sulfoxide, or glycerol, which also prevent aggregation. It appears that excess histidine may prevent aggregation by occupying the weak, axial positions. Upon freezing, two of the donor atoms that form the square plane are altered whereby two imidazole nitrogens, which may have been axial ligands, replace amine nitrogens and/or carboxyl oxygens. The histamine-like structure, Cu(His)$_2$, is the dominant species in the liquid phase (Figure 9b).

Often, nitrogen donor atoms from the imidazole moieties of histidine amino acid residues in proteins are bound to cupric ion. One question that is of primary interest to us is whether freezing the sample promotes substitution of nitrogen donor atoms from imidazole for nitrogen from amine, peptide linkages, or carboxyl groups. If nitorgen from imidazole favorably competes with other donor atoms as the temperature is lowered, structural information in the frozen state could be misleading.

It is reassuring that all simulations are consistent with a one to two stoichiometry for Cu(His)$_2$ in the liquid phase. Goodman et al.[10] found two complexes, one histamine-like for both ligands and the other histamine-like for one ligand and glycine-like for the second ligand, as do we. Future studies should focus on the pH and ligand concentration dependence.

The most convincing argument for four nitrogen donor atoms comes from the Fourier transform of the spectrum for Cu-2^{14}-N,2^{15}N (Figure 6). The lines obtained from the experimental data are shifted to lower frequency if two ^{15}N donor atoms and two ^{14}N donor atoms comprise the square plane. The reverse Fourier transforms are complicated. The best information comes from the outer lines, which correspond to the "highest frequency" pattern, i.e. the pattern with the smallest superhyperfine couplings. This pattern resembles the pattern expected from ^{14}N and ^{15}N (Table I). For example a nine-line pattern is obtained from the reverse Fourier transform from the experimental spectrum, Cu-^{14}N-exptl, and simulated spectrum, Cu-4^{14}N; a seven-line pattern is obtained from the simulation for Cu-3^{14}N; a seven-line pattern is obtained for the experimental data for Cu-^{14}N,^{15}N and for the simulated data for Cu-2^{14}N,2^{15}N; and an eight-line pattern is obtained for the simulated data for Cu-2^{14}N,^{15}N. Because the copper hyperfine lines are suppressed in the reverse Fourier transform, the number of lines in the reverse Fourier transform is one-fourth the number of lines in the simulated spectra. The simplified pattern is much easier to analyze than the original spectrum. The outermost peak in the spectrum for the Fourier transform domain and the pattern of its reverse Fourier transform are therefore diagnostic for the nitrogen hyperfine pattern (Table I). It is anticipated that the Fourier transform and reverse Fourier transform will be useful displays to unravel hyperfine coupling constants for spectra that are well resolved but complicated due to overlap of many lines. We plan to test these methods on the $g_\perp$ region of immobilized copper square-planar complexes for which the magnitudes of the hyperfine couplings for copper and nitrogen are both about 15 G.

Registry No. N_2, 7727-37-9; Cu(His)$_2$, 16884-54-1.

Contribution from the Department of Chemistry,
Seoul National University, Seoul 151, Republic of Korea

Kinetics and Mechanism of the Metal Ion Catalyzed Hydrolysis of Acetylpyridine Ketoxime Pyridinecarboxylates

Junghun Suh,* Byung Nam Kwon, Woo Young Lee, and Sae Hee Chang

Received July 30, 1986

The kinetics of the Cu(II)- or Zn(II)-catalyzed hydrolysis of 2- and 3-acetylpyridine ketoxime esters of picolinic acid or nicotinic acid were studied. Analysis of the kinetic data revealed that the picolinyl pyridine of 2-acetylpyridine ketoxime picolinate (**2a**) does not act as a general-base catalyst but exerts only electronic effects. Thus, the metal ions bind at the oxime moiety in the hydrolysis of **2a** as well as 2-acetylpyridine ketoxime nicotinate and the metal-bound nucleophiles attack the ester linkage. On the other hand, the metal ions catalyze the hydrolysis of picolinyl esters containing 3-acetylpyridine ketoxime or *p*-nitrophenol leaving groups by binding at the ester carbonyl oxygen through chelation at the picolinyl moiety. The kinetic data obtained in this study indicate that these two mechanisms are comparably efficient in terms of the reactivity of the metal–substrate complexes.

Metal ions catalyze some organic reactions by participating as Lewis acids. Elucidation of the catalytic roles of metal ions in these reactions provides important information on both inorganic and organic reactions.[1-3] In addition, possible catalytic roles of metal ions in the action of metalloenzymes can be disclosed by the mechanistic studies of small model compounds.

Previously, we performed several kinetic studies on the Cu(II)- or Zn(II)-catalyzed hydrolysis of oxime esters **1a,b**.[4-6] The

(1) Satchell, D. P. N.; Satchell, R. S. *Annu. Rep. Prog. Chem., Sect. A: Inorg. Chem.* **1979**, *75*, 25 and references therein.
(2) Dunn, M. F. *Struct. Bonding (Berlin)* **1975**, *23*, 61.
(3) Hipp, C. J.; Busch, D. H. *Coordination Chemistry*; Martell, A. E., Ed.; ACS Monograph 174; American Chemical Society: Washington, DC, 1978; Vol. 2, Chapter 2.

0020-1669/87/1326-0805$01.50/0